Bioactive Materials 2 (2017) 35–43

Contents lists available at ScienceDirect

Bioactive Materials

journal homepage: http://www.keaipublishing.com/en/journals/bioactive-materials/

Influence of mixed organosilane coatings with variable RGD surface densities on the adhesion and proliferation of human osteosarcoma Saos-2 cells to magnesium alloy AZ31

Xiaoxi Yang, Afrah Al Hegy, Eric R. Gauthier, Joy Gray-Munro*

Dept. of Chemistry and Biochemistry, Laurentian University, Sudbury, Ontario, P3E 2C6, Canada

ARTICLE INFO

Article history:
Received 17 November 2016
Received in revised form
18 January 2017
Accepted 19 January 2017
Available online 27 January 2017

Keywords:
Magnesium alloys
Biodegradable
Biomimetic
RGD peptide
Surface modification
Cell adhesion
Organosilane

ABSTRACT

In the last decade, the use of magnesium and its alloys as biodegradable implant materials has become increasingly accepted. However, surface modification of these materials to control the degradation rate in the early stages of healing and improve their biocompatibility is crucial to the successful implementation of magnesium alloy implants in medicine. Cell adhesion and proliferation at the implant surface is a vital factor for successful integration of a biomaterial within the body. Cells accomplish this task by binding to ligands such as the arginine-glycine-aspartic acid peptide sequence (RGD) commonly found on adhesive proteins present in the extracellular matrix. In this paper, we report a biomimetic surface modification strategy involving deposition of a mixed organosilane layer on Mg AZ31 followed by covalent immobilization of RGD peptides through a heterobifunctional cross-linker molecule. Our results indicate that with optimized deposition conditions uniform organosilane coatings were successfully deposited on the Mg AZ31 substrate. Furthermore, we have demonstrated that the surface density of immobilized RGD can be varied by depositing organosilane layers from solutions containing two different organosilanes in specified ratios. Increases in cell adhesion and cell proliferation were observed on the surface modified substrates.

1. Introduction

In the last decade, the use of magnesium and its alloys as a biodegradable orthopedic implant material has become increasingly accepted. They are considered an ideal candidate for this purpose due to their desirable mechanical properties [1–3] and the important role of magnesium in the body [4–7]. Several recent studies on the *in vitro* and *in vivo* performance of these materials indicate that in addition to being non-toxic, magnesium based implants exhibit good biocompatibility, osteoconductivity and osseointegrative properties [8–14]. However, the major drawback to the use of magnesium materials as orthopedic implants is their poor corrosion resistance in chloride containing environments leading to fast degradation along with the production of large volumes of hydrogen gas [10]. This process has a negative impact on the mechanical integrity of the implant leading to loss of implant stability before the impaired bone tissue has sufficiently healed and poor osteointegration of the magnesium implant [9,10,13]. In order to control the corrosion rate and extend the functional lifetime of magnesium implants in the human body, appropriate coatings with excellent adhesion as well as the ability to enhance the biocompatibility and slow the corrosion rate are crucial [15].

Organosilane coatings provide a unique opportunity to provide both the necessary corrosion resistance and the ability to biofunctionalize the magnesium implant surface. In particular, trialkoxysilanes have been commonly used as coupling agents to produce covalent bonds between organic and inorganic materials [16–19]. The general structure of a trialkoxysilane is $RSi(OR')_3$, where R′ is typically an alkyl group such as $-CH_3$ or $-CH_2CH_3$ and R is an organofunctional substituent that typically has a hydrocarbon bridge, $(-CH_2-)_n$, linked to the central silicon atom through an Si–C bond and terminated with a specific functional group [16]. An appropriate choice of functional group allows covalent immobilization of biomolecules of interest [16,17,19,20]. Under appropriate reaction conditions, a series of hydrolysis and condensation

* Corresponding author.
E-mail address: jgray@laurentian.ca (J. Gray-Munro).
Peer review under responsibility of KeAi Communications Co., Ltd.

http://dx.doi.org/10.1016/j.bioactmat.2017.01.001

reactions leads to a stable multilayer coating of cross-linked polysiloxane molecules that are also covalently bonded to the metal surface. Based on previous research, a thiol terminated organosilane, (3-Mercaptopropyl)trimethoxysilane (MPTS) can act as a water barrier coating to improve corrosion resistance [16,17,21,22]. In addition, the thiol functional group of MPTS provides reactive sites for the covalent immobilization of functional biomolecules [23].

For orthopedic implants, it is essential to establish a surface that is osteoconductive and osteoinductive and does not lead to fibrous tissue formation [24]. For most types of adherent cells, cell adhesion generally depends on the interaction between ligands in the extracellular matrix (ECM) and the corresponding integrin receptors on the cell surface; this process is essential for cell survival of non-malignant cells [25,26]. The arginylglycylaspartic acid (RGD) amino acid sequence has been found in a number of extracellular molecules, and this specific tri-peptide has been shown to play a key role in cell attachment [27–29]. Thus an appropriate surface modification that immobilizes RGD containing peptides to a substrate should improve cell-surface adhesion onto biomaterials [30–34]. Furthermore, Hu et al. also demonstrated that the presence of the RGD sequence can enhance the differentiation of osteogenic cells [35]. Although immobilizing the RGD-containing sequence to a substrate surface can efficiently mimic the natural ECM environment and significantly enhance cell adhesion to substrate surfaces there are still some differences in comparison to the natural ECM. For example, the RGD surface density, orientation and distribution have been shown to have an effect on cell adhesion, cell spreading and cell proliferation [36–39].

The main objective of this study was to develop a surface modification strategy for Mg AZ31 that gives controlled degradation rates and improved cell/surface interactions. Organosilane coatings with different thiol surface densities were prepared by varying the ratio of two different organosilanes, MPTS and tetraethoxysilane (TEOS), in the coating solution. A heterobifunctional crosslinker was used to covalently immobilize the RGD peptide to the thiol functional groups, resulting in coatings with variable RGD surface densities. The proposed surface modification procedure is illustrated in Fig. 1. The influence of MPTS/TEOS ratio on the surface chemistry, corrosion resistance and biocompatibility of the surface modified Mg AZ31 was evaluated.

2. Experimental details

2.1. Materials

Mg AZ31 foil (1 mm thickness) and 3-Maleimidopropionic acid N-hydroxysuccinimide ester (SMP) were purchased from Alfa Aesar (US). 3-Mercaptopropyltrimethoxysilane (MPTS), Tetraethoxysilane (TEOS), N,N-Dimethylformamide (DMF), Sodium Hydroxide, Arginylglycylaspartic acid (RGD) and gold nanoparticle suspension were purchased from Sigma-Aldrich (Canada). Sulfuric acid and Trypan Blue were purchased from Fisher Scientific (Canada). Phosphate Buffered Saline (PBS) (1x), McCoy's 5a, Trypsin EDTA (1X) and Fetal Bovine Serum (FBS) were purchased from Corning (Canada). Penicillin-Streptomycin Solution was purchased from HyClone (Canada). CyQUANT Cell Proliferation Assay was purchased from Life technologies (Canada). Acetone (reagent grade) was purchased from Caledon Laboratory Chemicals (Canada). Ethyl alcohol (95%) and methanol were purchased from Commercial Alcohols (Canada). All chemicals were used as received without further purification. The Saos-2 cell line was purchased from American Type Culture Collection (US) and cultured for further experiments.

2.2. Preparation of silanized Mg AZ31

Organosilane solutions were prepared with 3 different volume ratios of MPTS to TEOS including 1:1, 3:1 and pure MPTS while keeping the total volume of organosilane in the coating solution constant as described in Table 1. The pH of all silane solutions was adjusted to 4.20 by dropwise addition of 0.1 M H_2SO_4 immediately after mixing of the organosilane/water/methanol mixture. All solutions were aged with stirring for 7 h to ensure complete hydrolysis and optimum conditions for condensation of the silanol groups with hydroxyl groups on the substrate surface.

Mg AZ31 foil was machined into 1 cm diameter circular samples. The samples were polished to a 1 μm mirror finish with a diamond polishing suspension; AutoMet lapping oil (Buehler, Canada) was used as the lubricant. The polished AZ31 coupons were sonicated for 15 min in acetone and then rinsed well with deionized water for 5 min. The polished, degreased coupons were immersed in 0.05 M NaOH solution at 50 °C for 1 h, rinsed with copious amounts of deionized water and immediately air-dried. Each coupon was immersed in 25 ml of organosilane solution at 50 °C without stirring for 20 h. The coated coupons were removed from solution, immediately air-dried and then cured in an oven at 100 °C for 1 h.

2.3. Study of distribution of thiol functional groups

It is well documented that gold nanoparticles (AuNP) can specifically bond to thiol functional groups [40,41]. Therefore, each of the three coating types was exposed to 400 μl of a 10 nm diameter citrate stabilized AuNP suspension to evaluate the distribution of the thiol functional groups at the coating surface. After 1 h, the samples were removed from the AuNP suspension, rinsed with deionized water three times and immediately air-dried. A control group was also prepared by exposing the three coatings to a sodium citrate solution under the same conditions. The surface topographies of the coatings before and after treatment were evaluated by atomic force microscopy (AFM). This experiment was repeated 3 times.

2.4. Magnesium ion release rate – immersion test in 3.5% NaCl

The magnesium ion release rate of the coated samples compared to uncoated Mg AZ31 was evaluated by monitoring the concentration of magnesium in solution as a function of time upon immersion in 0.9% (w/v) NaCl solution at room temperature. The samples were mounted in epoxy with only the coated surface exposed to ensure a constant surface area from sample to sample. Each sample was immersed in 50 ml of NaCl solution. After 1, 3, 5, 7 and 14 days, the solutions were mixed well, a 100 μl aliquot was removed and diluted to 10 ml in a 2% nitric acid solution. The concentration of magnesium in the diluted solutions was determined using a Perkin Elmer AAnalyst flame atomic absorbance spectrometer (285.21 nm, air/acetylene flame).

2.5. Immobilization of the RGD peptide

The RGD peptide was covalently bonded through the surface thiol functional groups on the coated Mg AZ31 substrates using the heterobifunctional cross-linker SMP as previously described in the literature [23, 42]. Briefly, the SMP solution was prepared at a concentration of 5 mg/ml in dimethylformamide (DMF) and then diluted with pure ethanol to a final concentration of 1.7 mg/ml. Each silanized Mg AZ31 sample was exposed to 500 μl of freshly prepared SMP and allowed to react at room temperature for 1 h. After reaction with the crosslinker, the samples were rinsed three times with pure ethanol and once with deionized water to remove

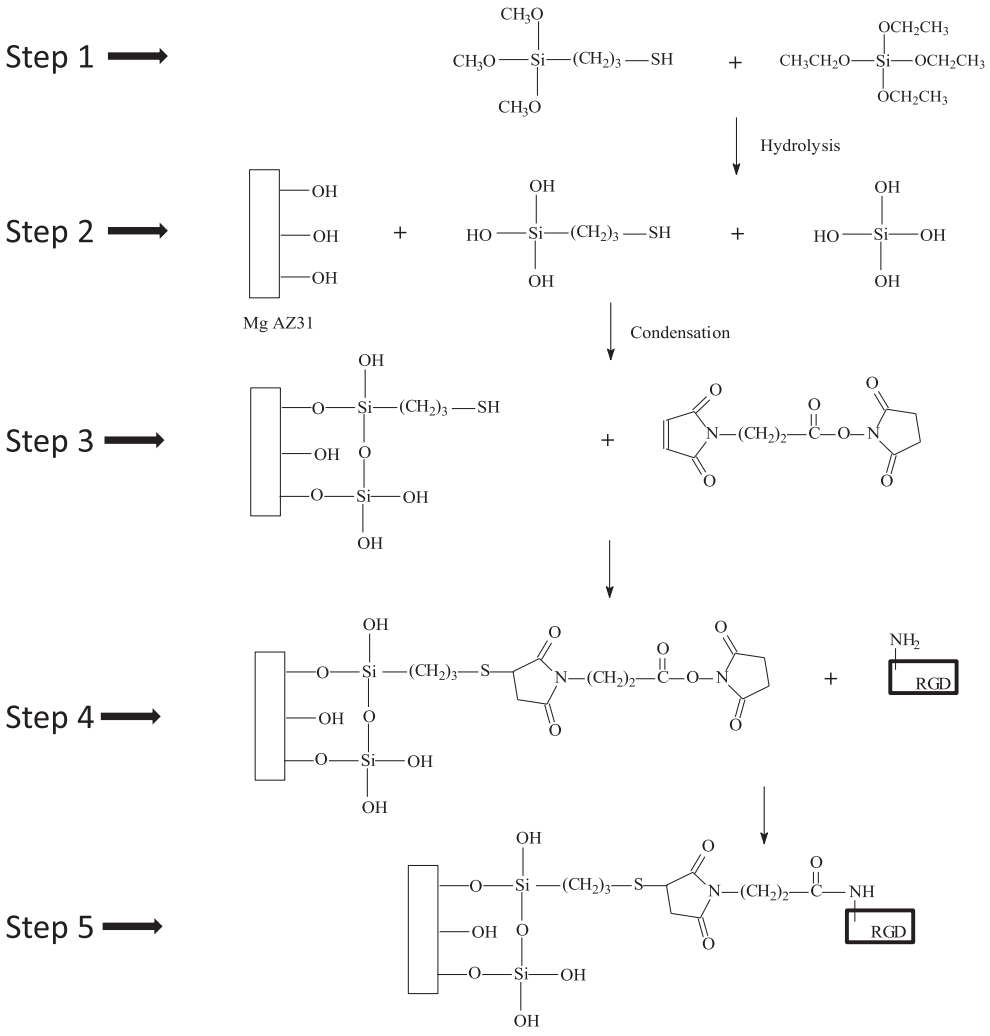

Fig. 1. Schematic representation of the surface modification strategy. Steps 1 and 2 illustrate the formation of the organosilane coating on the surface. Step 3 and 4 show the reaction of the heterobifunctional crosslinker with surface thiols and peptide amine groups. Step 5 is a schematic diagram of the final modified surface.

Table 1
Composition of coating solutions.

Coating solution	% MPTS (v/v)	% TEOS (v/v)	% H_2O (v/v)	% CH_3OH (v/v)	Mol % MPTS
MPTS/TEOS = 1	4%	4%	12%	80%	55%
MPTS/TEOS = 3	6%	2%	12%	80%	78%
MPTS	8%	0%	12%	80%	100%

non-bonded SMP molecules. The samples were immediately air-dried and then immersed in 400 μl of a 5 mg/ml RGD solution prepared by dissolving the peptide in warm PBS (1X). The RGD modified samples were rinsed with warm PBS solution 3 times to remove any non-bonded RGD molecules and immediately air-dried.

2.6. Surface characterization

2.6.1. Infrared spectroscopy

Infrared spectroscopy was performed with a Bruker Optics Hyperion infrared microscope equipped with an attenuated total reflectance objective (ATR-FTIR) with a germanium crystal. A liquid nitrogen cooled mercury cadmium telluride (MCT) detector was employed for all studies. The resolution of the spectrometer was 4 cm^{-1} and each spectrum was the result of 100 co-added scans. FTIR spectra were collected from three samples of each type at three different spots per sample (9 measurements/sample type). All presented spectra were baseline corrected and corrected for atmospheric CO_2 and H_2O with the OPUS software.

2.6.2. X-ray photoelectron spectroscopy (XPS)

XPS spectra were recorded on a Kratos Ultra spectrometer at the Alberta Centre for Surface Engineering and Science (ACSES), University of Alberta. The vacuum in the analytical chamber was less than 3×10^{-8} Pa. A monochromatic Al Kα source operated at 168 W was used and the analyzer resolution was 0.80 eV for Au 4f peaks. Two survey scans were recorded from 0 to 1100 eV at three different spots on each sample surface with a spot size of 300 × 700 μm. The relative concentrations of chemical elements were calculated using the CASAXPS software and a standard

quantification routine that included Schofield sensitivity factors and a Shirley background. The high resolution spectra have been corrected for charging by referencing the spectra to adventitious carbon at 284.8 eV.

2.6.3. Atomic force microscopy

Atomic force microscopy images were collected with a Bruker multimode III D AFM. The instrument was run in tapping mode using Bruker AFM TESPA probes. The cantilever probes had a resonant frequency of approximately 320 kHz. Images (10×10 μm) were collected at 512 samples/line and a scan rate of 0.5 Hz. The presented images are representative of the whole surface; each image was flattened using the software provided with the instrument.

2.6.4. Contact angle analysis

The geometric static contact angle of a 4 μL deionized water droplet (18 MΩ) with each surface was measured using a PG-2 Pocket Goniometer.

2.7. Cell culture

Human osteosarcoma Saos-2 cells, purchased from American Type Culture Collection, were cultured in McCoy's 5a cell culture medium containing 15% fetal bovine serum and 1% penicillin/streptomycin (hereafter designated McCoy's medium) at 37 °C in a 5% CO_2 atmosphere. The cell culture medium was refreshed every two days. The cells were detached from the flask with Trypsin/EDTA (Fisher Scientific), centrifuged at 2000 rpm for 5 min and resuspended in fresh McCoy's medium. The number of cells in the suspension was determined by the trypan blue dye exclusion assay using a Neubauer hemocytometer.

2.7.1. Cell adhesion on Mg AZ31 samples

Prior to the adhesion experiment, all samples were sterilized in 70% ethanol for 1 h followed by rinsing with warm, sterile PBS and allowed to dry in a laminar flow hood. The samples were then placed in the wells of a 24-well plate. In order to evaluate the capacity of RGD-modified Mg AZ31 to promote Saos-2 cell adhesion, 40,000 cells (in 600 μL McCoy's medium) were allowed to adhere on the substrates for 3 h at 37 °C in a 5% CO_2 atmosphere. Uncoated Mg AZ31 and organosilane-coated RGD-free samples were used as negative controls. After the incubation period, the samples were gently rinsed with warm PBS three times in order to remove non-adherent cells. Four hundred microliters of CyQUANT solution was added to each sample and incubated for 5 min. At the end of the incubation period, 100 μl of the CyQUANT solution was pipetted from each well to a black EIA/RIA 96-Well plate (Costar) and the fluorescence intensities of each solution was measured with a Fluostar OPTIMA fluorescence microplate reader. These values were compared to a calibration curve of cell number vs. fluorescence intensity for quantitative analysis.

The CyQuant dye only fluoresces when bound to nucleic acids (DNA) and does not exhibit a false positive in the presence of magnesium. This was confirmed through a control experiment that measured the fluorescence of the dye under the same experimental conditions but in the absence of cells.

2.7.2. Cell Proliferation Assay

RGD-modified and uncoated Mg AZ31 samples were sterilized as described above and placed in the wells of a 24-well plate. Five thousand cells (in 600 μL McCoy's medium) were seeded on the substrates and incubated at 37 °C in a 5% CO_2 atmosphere for 10 days. The cell culture medium was refreshed every two days. After the required incubation period, the number of cells on the substrates was measured using the CyQUANT assay kit as described above.

2.8. Statistical analysis

All quantitative data is presented as an average ± standard deviation of multiple trials. The number of samples tested in each case is indicated in the figure captions. Statistical significance of the observed differences in the cell adhesion and cell proliferation data was determined with a paired student t-test. A value of $p < 0.05$ was assumed to indicate significant differences.

3. Results

3.1. Characterization of the mixed organosilane coatings

3.1.1. ATR-FTIR results

A total of 9 ATR-FTIR (3 samples, 3 spots on each) spectra were collected for each coating deposited from solutions with MPTS/TEOS = 1, MPTS/TEOS = 3 and MPTS. In each case, the films were uniformly deposited across the surface of the Mg AZ31 substrates and the spectra were reproducible from sample to sample (results not shown). Fig. 2 shows representative ATR-FTIR spectra of the three different organosilane coatings. The Si—O peak at 1000—1100 cm^{-1} is indicative of the presence of organosilane on the surface. This peak is at similar peak intensity for all three coating types, suggesting that the overall coating thickness is comparable. In addition, a relative increase in the peak intensities for the Si—C peak at 1250 cm^{-1} and the S—H peak at 2550 cm^{-1} (Fig. 2 inset) was observed as the mol % of MPTS in the coating solution was increased. This confirms that the relative ratio of MPTS/TEOS in the deposited coating mirrors that of the coating solution and that mixed organosilane coatings with variable concentrations of the thiol functional group have been successfully prepared.

3.1.2. Surface chemistry and wettability

Fig. 3 shows the observed change in water contact angle and S/Si XPS ratio for the deposited coatings as a function of mol % of MPTS in the coating solution. A linear increase in the S/Si ratio confirms that the surface density of thiol groups increases as the mol % MPTS

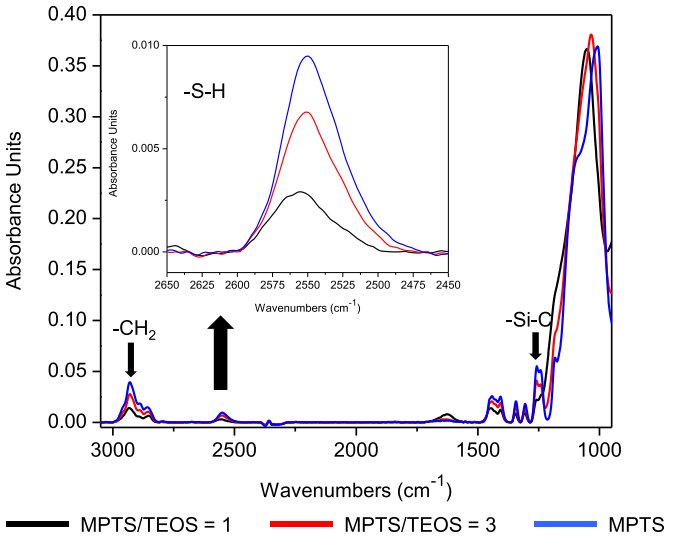

Fig. 2. spectra of organosilane coatings deposited on Mg AZ31 substrates from three different coating solutions.

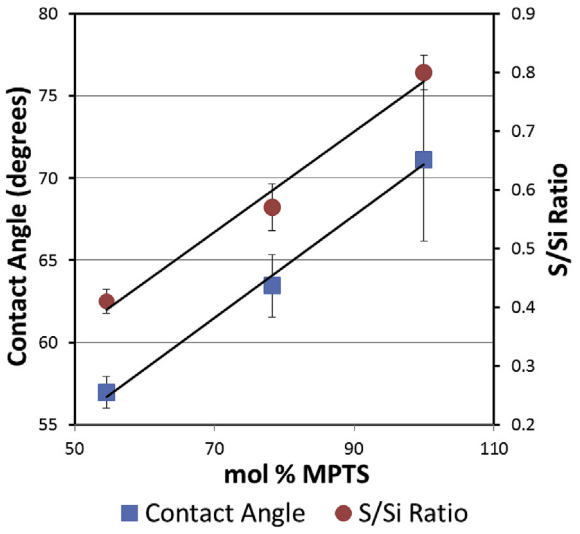

Fig. 3. XPS S/Si atomic % and water contact angle analysis of organosilane coatings deposited on Mg AZ31 substrates from three different coating solutions. XPS data are the average ± standard deviation of 3 measurements. Contact angles are the average ± standard deviation of a minimum of 6 measurements.

in the coating solution increased. The contact angle also increased linearly as a function of increasing S/Si ratio at the surface due to the hydrophobic nature of the thiol functionalized alkyl chain of the MPTS molecule. These results, coupled with the ATR-FTIR results (Fig. 2) confirm that a variation in MPTS/TEOS ratio in the coating solution translates into a controlled variation in the number of surface thiol groups available for subsequent reaction on the silanized surface.

3.1.3. *Atomic force microscopy results*

The topography of the deposited organosilane films and the overall distribution of the thiol groups at the coating surface were investigated using atomic force microscopy. Fig. 4 (a–c) shows the topography of the organosilane coatings with different MPTS/TEOS ratios prior to AuNP treatment. All three organosilane coatings were smooth and uniform at the 10 × 10 μm scale.

AFM images of the organosilane coated Mg AZ31 surfaces after AuNP treatment are presented in Fig. 4 (d–e). The coating prepared from a solution with MPTS/TEOS = 1 showed no significant difference after treatment with AuNPs (4 d). This may indicate that the thiol groups are randomly distributed across the surface since individual thiol molecules or regions with low thiol surface density may not provide sufficient binding sites to effectively tether AuNPs to the surface. In comparison, the AFM image for the MPTS coating exposed to the AuNPs (Fig. 4f) shows a completely new morphology consisting of a thick (at least 30 nm), smooth and uniform top-layer with a few cracks. In addition, some AuNP clusters can be observed within the layer. This uniform distribution of AuNPs is likely due to the high surface density of thiol groups on the pure MPTS coating. The most surprising result was obtained for the coating prepared from a solution with MPTS/TEOS = 3. A distinct pattern showing an interconnected network of AuNP clusters was observed (Fig. 4e). The observed surface structure is similar to that typically reported for the tapping mode phase images of phase segregated block copolymers suggesting that when the MPTS/TEOS ratio is high, phase separation of the two organosilanes occurs at the surface [43]. This may be due to the relative hydrophobicity of the hydrolyzed and condensed MPTS compared to that of TEOS. In order to confirm that the observed interconnected structure was due to AuNP adsorption and not simply dissolution of one phase of the organosilane coating over another, a control experiment was performed. The coating was treated with the citrate buffer solution (no AuNP's) under the same conditions. This phase separated structure was not seen in the control experiment confirming that the observed pattern is most likely due to adsorption of AuNP's to MPTS rich regions of the coating and that the thiols are not randomly distributed across the surface of the coating but are localized in MPTS rich domains of the organosilane coating.

The thickness of the coatings was also determined by atomic force microscopy. In this experiment half of the organosilane coating was dissolved from the surface with a 40% (v/v) hydrofluoric acid solution. This solution readily dissolves silicon based compounds but does dissolve magnesium. Atomic force microscopy

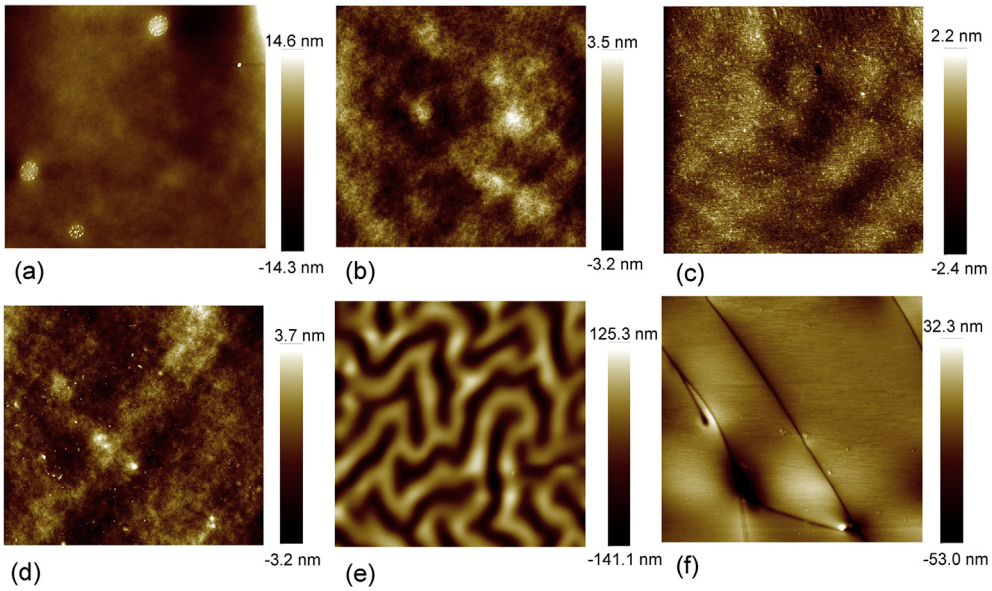

Fig. 4. 10 × 10 μm scale AFM images of organosilane coatings deposited on Mg AZ31 substrates from three different coating solutions before and after treatment with 10 nm gold nanoparticles (AuNP's). a) as-deposited coating MPTS/TEOS = 1, b) as-deposited coating MPTS/TEOS = 3, c) as-deposited coating MPTS, d) AuNP treated coating MPTS/TEOS = 1, e) AuNP treated coating MPTS/TEOS = 3 and f) AuNP treated coating MPTS.

images were collected at the edge of the coating and the thickness was estimated by determining the height difference from the edge of the coating to the bare magnesium substrate. All coatings were below 1 μm in thickness. The results are reported in Table 2.

3.2. Magnesium ion release rate

The ability of the 3 different coatings to control the degradation rate of the underlying magnesium alloy in an aqueous salt solution was quantified by determining the amount of magnesium dissolved as a function of sample immersion time in a 0.9% (w/v) NaCl solution. The coated and uncoated samples were immersed in the solution for up to 14 days. The reported values are an average of the magnesium levels detected in aliquots taken from the 0.9% (w/v) NaCl solution at various time points. The results are shown in Fig. 5. Up to the third day the magnesium ion release rate was low for all of the organosilane coatings in comparison to the uncoated substrate. However, by the fifth day it is evident that the coating with MPTS/TEOS = 1 is the least protective; the amount of magnesium dissolved is similar to that observed for the uncoated sample. In contrast, even after immersion in the 0.9% (w/v) NaCl solution for 14 days both the MPTS/TEOS = 3 and pure MPTS coatings exhibited improved resistance to degradation in comparison to uncoated magnesium.

3.3. XPS analysis of the RGD modified coatings

XPS analysis of the samples after RGD immobilization showed the presence of nitrogen at the surface for all coated samples. The high resolution N (1s) spectrum in Fig. 6b has been deconvoluted into two peaks at binding energies of 400.2 eV and 401.8 eV respectively. This is a close match to previous studies where the RGD peptide was reported to exhibit two peaks in its N (1s) high resolution spectrum due to amide bonds/guanidine group (400.1 eV) and protonated amine groups on the arginine residue (401.6 eV) [44] confirming that the RGD peptide was successfully immobilized to the organosilane surfaces. Fig. 6a is a graph of the N/S atomic % ratio for the three different coating types after covalent immobilization of the RGD peptide. The observed N/S ratio was similar for the two mixed organosilane coatings. However a large increase in N/S ratio was observed for the pure MPTS coating. This is due to the higher surface density of thiol groups available for reaction on the pure MPTS coating in comparison to the mixed films. This result demonstrates that it is possible to use mixed organosilane coatings to vary the surface density of the RGD peptide.

3.4. Cell adhesion assay

As shown in Fig. 7a, Saos-2 cells adhered on all silanized Mg AZ31 substrate surfaces but with varied efficiencies. Compared with uncoated Mg AZ31, a significant increase in cell adhesion was observed on all three silanized substrates. In addition, among the silanized Mg AZ31 substrates, the mixed organosilane coated surfaces performed the best in terms of cell adherence capacity. A statistically significant difference, $p < 0.05$, for the mixed organosilane coatings (MPTS/TEOS = 1 and MPTS/TEOS = 3) in comparison

Table 2
Mixed organosilane coating thickness.

Type of coating	Measured thickness
MPTS/TEOS = 1	696 ± 58
MPTS/TEOS = 3	658 ± 43
MPTS	938 ± 85

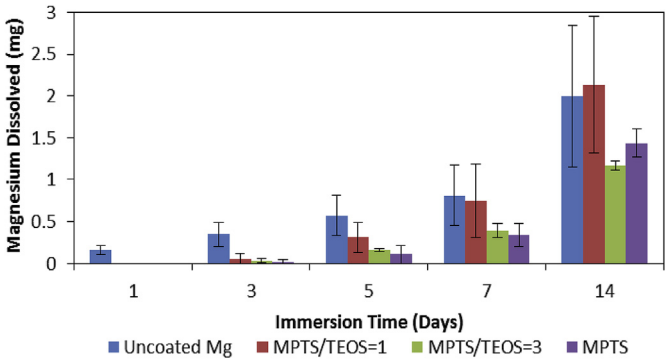

Fig. 5. Amount of magnesium dissolved in a 0.9% NaCl (w/v) solution as a function of immersion time for uncoated and coated Mg AZ31 samples. Data are the average ± standard deviation of at least 3 samples.

to the pure MPTS coating was observed with less cell adhesion on the pure MPTS coating. Fifteen to 38 times more adherent cells were observed on the silanized substrate surfaces than the uncoated Mg AZ31 control group. Compared with uncoated Mg AZ31, the higher cell adhesion capacities can be attributed to the presence of organosilane coatings which provided a layer of protection from corrosive attack in cell culture medium, and allowed cells to adhere on a stable physical surface. Corrosion of magnesium is accompanied by the evolution of hydrogen gas which likely physically inhibits cell adhesion. The decrease in cell adherence observed for the different silanized substrate surfaces might be related to the concentration of the different surface functional groups. In general, hydrophilic surfaces promote cell adhesion compared with hydrophobic surfaces [45]. In addition, Ertel et al. reported that a

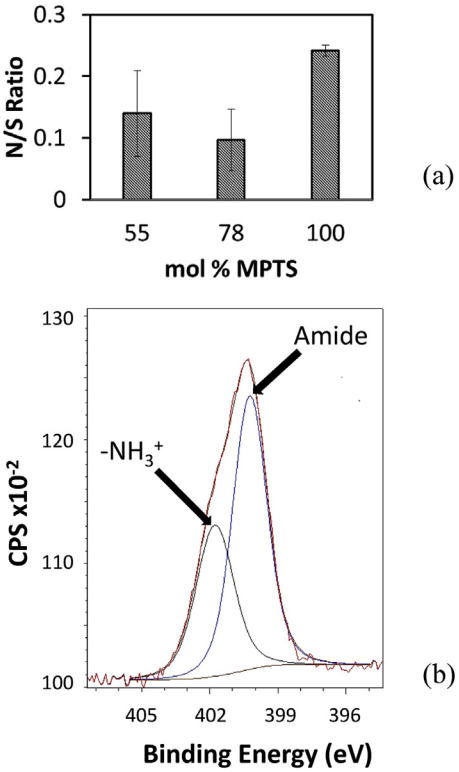

Fig. 6. XPS analysis of the RGD modified coatings. a) N/S atomic % for organosilane coatings deposited on Mg AZ31 substrates from three different coating solutions and b) high resolution N 1s spectrum for RGD modified MPTS coating. Quantitative data are the average ± standard deviation of 3 measurements.

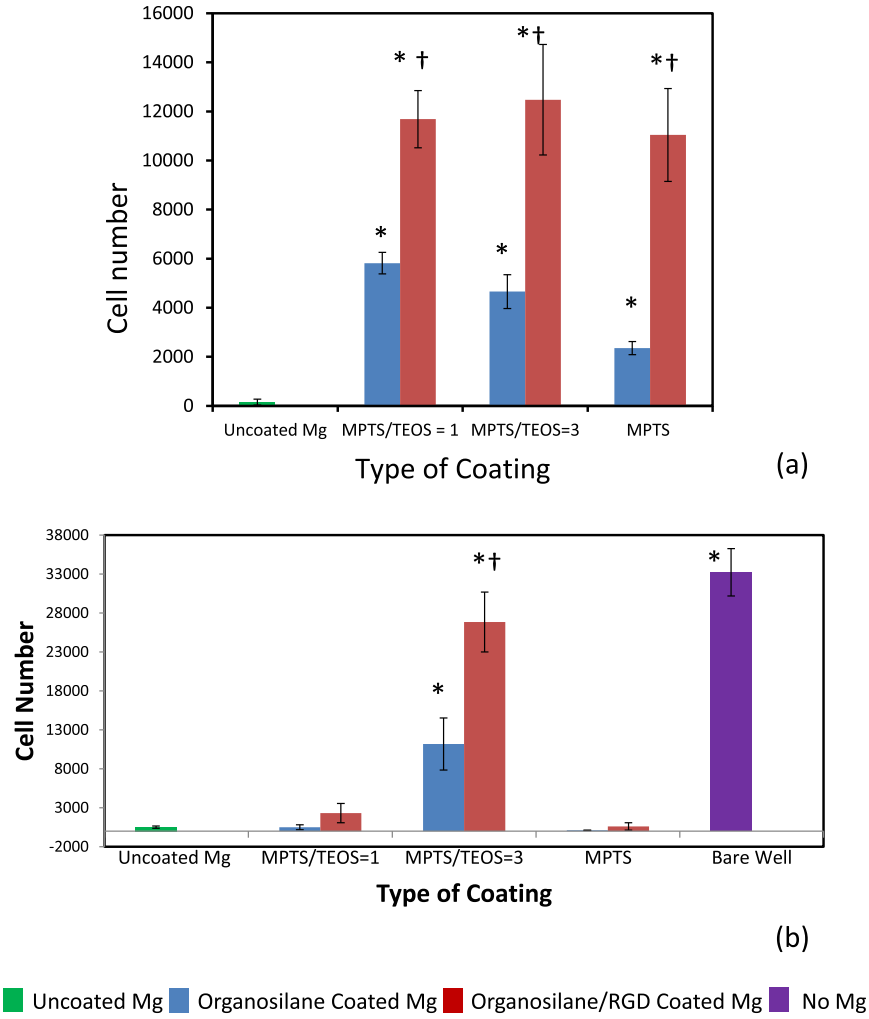

Fig. 7. Results of the cell adhesion and cell proliferation tests. a) number of Saos-2 cell adhered on uncoated Mg AZ31, organosilane coated Mg AZ31 and RGD modified organosilane coated Mg AZ31 surfaces after a 3 hour incubation period. Uncoated Mg AZ31 and organosilane coatings without RGD modification were applied as control groups. Data are the average ± standard deviation of 4 samples (2 replicates of 2 independent experiments) and b) Saos-2 cell proliferation numbers on uncoated Mg AZ31, organosilane coated Mg AZ31 and RGD modified organosilane coated Mg AZ31 surfaces after a 10 day proliferation time. Uncoated Mg AZ31, organosilane coatings without RGD modification were applied as control groups. In addition cell proliferation in the absence of any magnesium substrate (bare well) was measured Data are the average ± standard deviation of 4 samples (2 replicates of 2 independent experiments).* indicates $p<0.05$ between uncoated Mg and the sample. † indicates $p<0.05$ between organosilane coated Mg and organosilane/RGD coated Mg.

surface with high oxygen-containing functional groups enhances cell growth on a substrate [46]. In this regard, it is interesting to note that the observed decrease in Saos-2 cell adhesion correlated with the decrease in the −OH surface density from the mixed organosilane coatings to pure MPTS surfaces.

Fig. 7a also demonstrates that all three RGD-modified organosilane coated substrates recruited more Saos-2 cells than the control groups after a 3-h incubation period. Moreover, the adhered cell numbers were the same regardless of the RGD surface density. These results demonstrate that the chemically bonded RGD peptide acts as a bioactive ligand that stimulates cell/surface adhesion. However, the same level of cell adhesion to all RGD-modified substrates, regardless of surface density, indicates that differences in RGD surface density are not a critical factor for initial cell adhesion on these coatings.

3.5. Cell Proliferation Assay

Fig. 7b shows the cell number on the investigated substrates after 10 days. On uncoated Mg AZ31 and the MPTS/TEOS = 1 and pure MPTS organosilane coated substrates, the cell numbers were very low with no statistically significant between these groups ($p > 0.05$). Very few of the Saos-2 cells that had initially adhered to these organosilane coated surfaces (Fig. 7a) survived indicating that these silanized surfaces were not effective for long term cell adhesion and proliferation.

The highest cell proliferation rates were observed on the organosilane coated and RGD-modified organosilane coated substrates with MPTS/TEOS = 3. In fact, the number of cells on the MPTS/TEOS = 3 coated substrate modified with RGD approached the cell numbers observed for the positive control group (bare wells). These results indicate that the RGD modified protective coating deposited from a 3:1 mixed organosilane solution provided an appropriate environment for cell adhesion, survival and proliferation.

4. Discussion

When magnesium alloys degrade in an aqueous environment,

hydrogen gas is produced according to the generalized reaction below:

$$Mg(s) + 2H_2O(l) \rightarrow Mg(OH)_2(s) + H_2(g)\uparrow \quad (1)$$

In this study, cell adhesion and proliferation were both minimal on the uncoated Mg AZ31 surface. This can be directly attributed to the instability of the magnesium alloy surface in aqueous environments resulting in concomitant dissolution of the surface itself and the production of hydrogen gas bubbles. This unstable surface, coupled with the presence of hydrogen gas bubbles, both act to impede cell adhesion resulting in poor biocompatibility of the uncoated surface. The low proliferation capacity of Saos-2 cells on RGD-modified MPTS/TEOS = 1 substrates might be related to the low RGD surface density which does not provide sufficient cell adhesion sites for strong Saos-2 cell binding. Therefore, after initial cell adhesion, Saos-2 cells detach from these substrates, resulting in low Saos-2 cell proliferation. In addition, the relatively high magnesium ion release rate and concomitant increase in pH at the Mg alloy/solution interface for this surface results in an unstable environment for cell survival, proliferation and other complex cell behaviors.

On the other hand, although the RGD-modified pure MPTS substrates showed the highest RGD surface density their cell proliferation capacity was low. Previous studies have shown that the surface density of RGD peptides plays an important role in cell/substrate interactions which can further influence the signal pathways for cell behaviors on substrates [28,37–39]. In general an increase in RGD surface density has been shown to increase cell adhesion however it has also been observed that high surface densities of RGD lead to steric crowding impeding the interaction between cell and the RGD ligands [39].

In this study, a significant enhancement in the biocompatibility of Mg AZ31 coated with an RGD modified MPTS/TEOS = 3 coating was observed. This may be attributed to a combination of improved surface stability due to a decreased degradation rate as well as an optimum RGD surface density. Although the coating does not fully prevent corrosion of the underlying magnesium substrate, various studies have demonstrated that the presence of bivalent cations, such as Mg^{2+}, Ca^{2+}, Mn^{2+}, increase the integrin/ligand recognition and positively influence cell adhesion. In addition, a number of studies have reported that Mg^{2+} plays an essential role in cell proliferation and differentiation [4,47]. Low extracellular Mg^{2+} concentrations have been shown to inhibit the proliferation of osteoblastic cell lines [48] while high extracellular Mg^{2+} concentration induces the synthesis of DNA and proteins thus stimulating cell division [4]. It has also been demonstrated that the bioceramic, Al_2O_3, modified with Mg^{2+} has improved biocompatibility compared to the unmodified material due to an increase in the levels of $\alpha_5\beta_1$-and β_1-integrins on the cell surface promoted by the presence of Mg^{2+} on the surface [47].

5. Conclusions

In this paper, a simple immersion method for depositing mixed organosilane coatings with variable surface thiol densities was reported. At optimal organosilane concentration and deposition time, three organosilane coatings with different MPTS to TEOS ratios were successfully and uniformly deposited on Mg AZ31. All three coating types exhibited a decreased degradation rate compared to the bare substrate. In addition, the cell adhesion tests indicated that the presence of immobilized RGD peptides increased the adhesion of Saos-2 cell on Mg AZ31 substrates compared with either bare or silanized biomaterials. However, there was no significant difference in cell adhesion as a function of RGD surface density. Interestingly, increased cell proliferation was only observed on the MPTS/TEOS = 3 coated Mg AZ31 substrates with RGD modification. The results of this study suggest that surfaces with optimized RGD surface density and magnesium ion release rate lead to improved biocompatibility of magnesium substrates. This paper illustrates the importance of developing surface modification strategies for biodegradable magnesium alloys that control both the degradation rate and the cell/surface interactions in order to optimize the biocompatibility of these materials.

Acknowledgements

The authors gratefully acknowledge the support of the Natural Sciences and Engineering Research Council of Canada (RGPIN/298348-2010) and the Laurentian University Research Fund.

References

[1] M.P. Staigera, A.M. Pietaka, J. Huadmaia, G. Dias, Magnesium and its alloys as orthopedic biomaterials: a review, Biomaterials 27 (2006) 1728–1734.
[2] G. Song, Control of biodegradation of biocompatable magnesium alloys, Corros. Sci. 49 (2007) 1696–1702.
[3] F. Witte, V. Kaese, H. Haferkamp, E. Switzer, A. Meyer-Lindenberg, C.J. Wirth, H. Windhagen, In vivo corrosion of four magnesium alloys and the associated bone response, Biomaterials 26 (2005) 3557–3563.
[4] F.I. Wolf, A. Cittadini, Magnesium in cell proliferation and differentiation, Front. Biosci. 4 (1991) 607–617.
[5] C. Fox, D. Ramsoomair, C. Carter, Magnesium: its proven and potential clinical significance, South. Med. J. 19 (2001) 1195–1201.
[6] H. Rubin, Central role for magnesium in coordinate control of metabolism and growth in animal cells, Proc. Natl. Acad. Sci. U. S. A. 72 (1975) 3551–3555.
[7] A. Hartwig, Role of magnesium in genomic stability, Mutat. Res-Fund. Mol. M. 475 (2001) 113–121.
[8] A. Pietak, P. Mahoney, G.J. Dias, M.P. Staiger, Bone-like matrix formation on magnesium and magnesium alloys, J. Mater. Sci.-Mater. M. 19 (2008) 407–415.
[9] T. Kraus, S.F. Fischerauer, A.C. Hänz, P.J. Uggowitzer, J.F. Löffler, A.M. Weinber, Magnesium alloys for temporary implants in osteosynthesis: in vivo studies of their degradation and interaction with bone, Acta Biomater. 8 (2012) 1230–1238.
[10] H. Kuwahara, Y. Al-Abdullat, N. Mazaki, S. Tsutsumi, T. Aizawa, Precipitation of magnesium apatite on pure magnesium surface during immersing in Hank's solution, Mater. Trans. 42 (2001) 1317–1321.
[11] L. Xu, G. Yu, E. Zhang, F. Pan, K. Yang, In vivo corrosion behavior of Mg-Mn-Zn alloy for bone implant application, J. Biomed. Mater. Res. A 83 (2007) 703–711.
[12] E. Zhang, L. Xu, G. Yu, F. Pan, K. Yang, In vivo evaluation of biodegradable magnesium alloy bone implant in the first 6 months implantation, J. Biomed. Mater. Res. A 90 (2009) 882–893.
[13] F. Witte, V. Kaese, H. Haferkamp, E. Switzer, A. Meyer-Lindenberg, C.J. Wirth, H. Windhagen, In vivo corrosion of four magnesium alloys and the associated bone response, Biomaterials 26 (2005) 3557–3563.
[14] Z. Li, X. Gu, S. Lou, Y. Zheng, The development of binary Mg-Ca alloys for use as biodegradable materials within bone, Biomaterials 29 (2008) 1329–1344.
[15] D. Xue, Z. Tan, M.J. Schulz, W.J. Vanooija, J. Sankar, Y. Yuna, Z. Dong, Corrosion studies of modified organosilane coated magnesium–yttrium alloy in different environments, Mater. Sci. Eng. C 32 (2012) 1230–1236.
[16] A. Scott, J.E. Gray-Munro, The surface chemistry of 3-mercaptopropyltrimethoxysilane films deposited on magnesium alloy AZ91, Thin Solid Films 517 (2009) 6809–6816.
[17] A.F. Scott, J.E. Gray-Munro, J.L. Shepherd, Influence of coating bath chemistry on the deposition of 3-mercaptopropyl trimethoxysilane films deposited on magnesium alloy, J. Colloid Interf. Sci. 343 (2010) 474–483.
[18] A. Najari, P. Lang, P.C. Lacaze, D. Mauer, Adsorption of γ-mercaptopropyltrimethoxysilane on zinc: a study of the competition between thiol and silanol functions related to the age of the siloxane solution, its pH and the oxidation state of the surface, Surf. Sci. 606 (2012) 137–145.
[19] D.A. Ramrus, J.C. Berg, Characterization and adhesion testing of mixed silane-treated surfaces, J. Adhes. Sci. Technol. 18 (2004) 1395–1414.
[20] J.P. Matinlinna, K. Laajalehto, T. Laiho, I. Kangasniemi, L.V.J. Lassila, P.K. Vallittu, Surface analysis of Co–Cr–Mo alloy and Ti substrates silanized with trialkoxysilanes and silane mixtures, Surf. Interface Anal. 36 (2004) 246–253.
[21] W.E.G. Hansal, S. Hansal, M. Pölzler, A. Kornherr, G. Zifferer, G.E. Nauer, Investigation of polysiloxane coatings as corrosion inhibitors of zinc surfaces, Surf. Coat. Tech. 200 (2006) 3056–3063.
[22] P.R. Underhill, D.L. Duquesnay, Corrosion resistance imparted to aluminum by silane coupling agents, Silanes Other Coupling Agents 2 (2000) 149–158.
[23] S.K. Bhatia, L.C. Shriver-Lake, K.J. Prior, J.H. Georger, J.M. Calvert, R. Bredehorst,

F.S. Ligler, Use of thiol-terminal silanes and heterobifunctional crosslinkers for immobilization of antibodies on silica surfaces, Anal. Biochem. 178 (1989) 408–413.
[24] T. Albrektsson, C. Johansson, Osteoinduction, osteoconduction and osseointegration, Eur. Spine J. 10 (2001) 96–101.
[25] C.J. Wilson, R.E. Clegg, D.I. Leavesley, M.J. Pearcy, Mediation of biomaterial-cell interactions by adsorbed proteins: a review, Tissue Eng. 11 (2005) 1–18.
[26] S. Gronthos, P.J. Simmons, S.E. Graves, P.G. Robey, Integrin-mediated interactions between human bone marrow stromal precursor cells and the extracellular matrix, Bone 28 (2001) 174–181.
[27] R.G. LeBaron, K.A. Athanasiou, Extracellular matrix cell adhesion peptides: functional applications in orthopedic materials, Tissue Eng. 6 (2000) 85–103.
[28] U. Hersel, C. Dahmen, H. Kessler, RGD modified polymers: biomaterials for stimulated cell adhesion and beyond, Biomaterials 24 (2003) 4385–4415.
[29] A. Hautanen, J. Gailit, D.M. Mann, E. Ruoslahti, Effects of modifications of the RGD sequence and its context on recognition by the fibronectin receptor, J. Biol. Chem. 264 (1989) 1437–1442.
[30] D.A. Puleo, R. Bizios, RGDS tetrapeptide binds to osteoblasts and inhibits fibronectin-mediated adhesion, Bone 12 (1991) 271–276.
[31] A.J. García, P. Ducheyne, D. Boettiger, Effect of surface reaction stage on fibronectin-mediated adhesion of osteoblast-like cells to bioactive glass, J. Biomed. Mater. Res. 40 (1998) 48–56.
[32] K.L. Kilpadi, A.A. Sawyer, C.W. Prince, P. Chang, S.L. Bellis, Primary human marrow stromal cells and Saos-2 osteosarcoma cells use different mechanisms to adhere to hydroxylapatite, J. Biomed. Mater. Res. A 68A (2004) 273–285.
[33] A. Bagno, A. Piovan, M. Dettin, A. Chiarion, P. Brun, R. Gambaretto, G. Fontana, C. Di Bello, G. Palù, I. Castagliuolo, Human osteoblast-like cell adhesion on titanium substrates covalently functionalized with synthetic peptides, Bone 40 (2007) 693–699.
[34] E.S. Gawalt, M.J. Avaltroni, M.P. Danahy, B.M. Silverman, E.L. Hanson, K.S. Midwood, J.E. Schwarzbauer, J. Schwartz, Bonding organics to Ti alloys: facilitating human osteoblast attachment and spreading on surgical implant materials, Langmuir 19 (2003) 200–204.
[35] Y. Hu, S.R. Winn, I. Krajbich, J.O. Hollinger, Porous polymer scaffolds surface-modified with arginine-glycine-aspartic acid enhance bone cell attachment and differentiation in vitro, J. Biomed. Mater. Res. A 64A (2003) 583–590.
[36] E.J. Tocce, A.H. Broderick, K.C. Murphy, S.J. Liliensiek, C.J. Murphy, D.M. Lynn, P.F. Nealey, Functionalization of reactive polymer multilayers with RGD and an antifouling motif: RGD density provides control over human corneal epithelial cell–substrate interactions, J. Biomed. Mater. Res. A 100A (2012) 84–93.
[37] S. Inouea, Y. Iida, Y. Otani, Y. Hirano, Y. Tabata, Adhesion behavior of human adipo-stromal cells on self-assembled monolayers with different surface densities or gradients of RGD peptide, J. Biomater. Sci.-Polym. E. 20 (2009) 495–510.
[38] C. Chollet, C. Chanseau, M. Remy, A. Guignandon, R. Bareille, C. Labrugère, L. Bordenave, M.C. Durrieu, The effect of RGD density on osteoblast and endothelial cell behavior on RGD-grafted polyethylene terephthalate surfaces, Biomaterials 30 (2009) 711–720.
[39] G. Le Saux, A. Magenau, T. Böcking, K. Gaus, J.J. Gooding, The relative importance of topography and RGD ligand density for endothelial cell adhesion, PLoS One 6 (2011) e21869.
[40] M.C. Daniel, D. Astruc, Gold nanoparticles: assembly, supramolecular chemistry, quantum-size-related properties, and applications toward biology, catalysis, and nanotechnology, Chem. Rev. 104 (2004) 293–346.
[41] I. Byun, A.W. Coleman, B. Kim, Transfer of thin Au films to polydimethylsiloxane (PDMS) with reliable bonding using (3-mercaptopropyl) trimethoxysilane (MPTMS) as a molecular adhesive, J. Micromech. Microeng. 23 (2013) 085016.
[42] S.J. Xiao, M. Textor, N.D. Spencer, Covalent attachment of cell-adhesive, (Arg-Gly-Asp)-Containing peptides to titanium surfaces, Langmuir 14 (1998) 5507–5516.
[43] F.S. Bates, G.H. Fredrickson, Block copolymer thermodynamics: theory and experiment, Annu. Rev. Phys. Chem. 41 (1990) 525–557.
[44] J.S. Stevens, A.C. de Luca, M. Pelendritis, G. Terenghi, S. Downes, S.L.M. Schroeder, Quantitative analysis of complex amino acids and RGD peptides by X-ray photoelectron spectroscopy (XPS), Surf. Interface Anal. 45 (2013) 1238–1246.
[45] K. Anselme, Osteoblast adhesion on biomaterials, Biomaterials 21 (2000) 667–681.
[46] P. Thevenot, W. Hu, L. Tang, Surface chemistry influences implant biocompatibility, Curr. Top. Med. Chem. 8 (2008) 270–280.
[47] H. Zreiqat1, C.R. Howlett, A. Zannettino, P. Evans, G. Schulze-Tanzil, C. Knabe, M. Shakibaei, Mechanisms of magnesium-stimulated adhesion of osteoblastic cells to commonly used orthopaedic implants, J. Biomed. Mater. Res. 62 (2002) 175–184.
[48] E. Abed, R. Moreau, Importance of melastatin-like transient receptor potential 7 and cations (magnesium, calcium) in human osteoblast-like cell proliferation, Cell Proliferat. 40 (2007) 849–865.